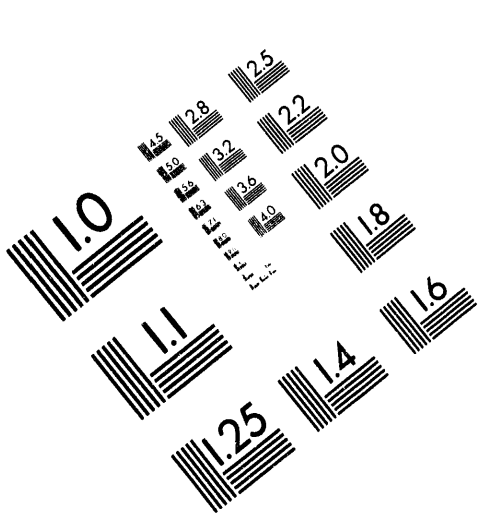

Association for Information and Image Management

1100 Wayne Avenue, Suite 1100
Silver Spring, Maryland 20910

301/587-8202

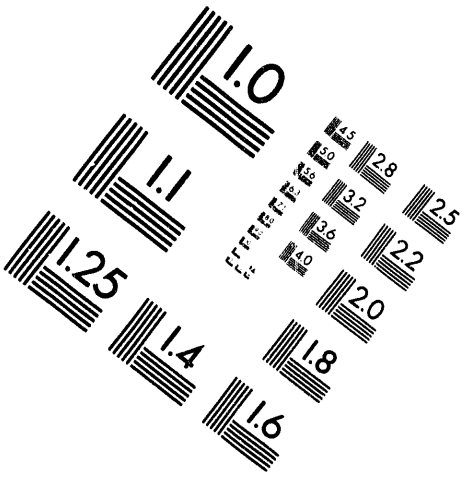

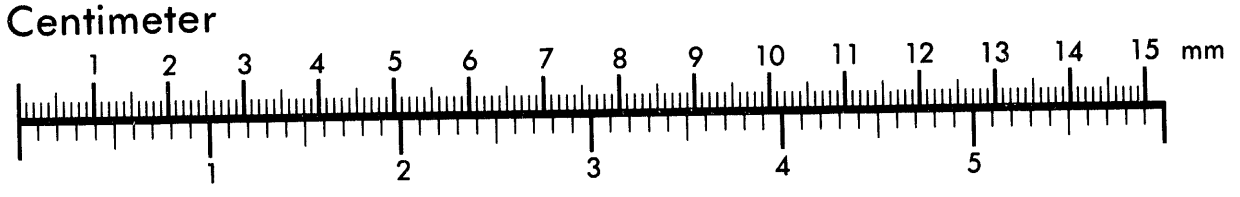

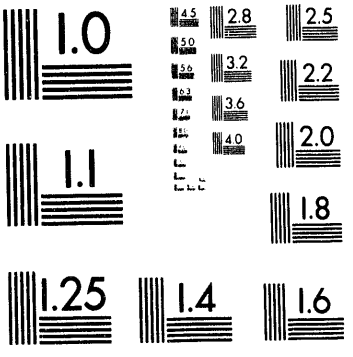

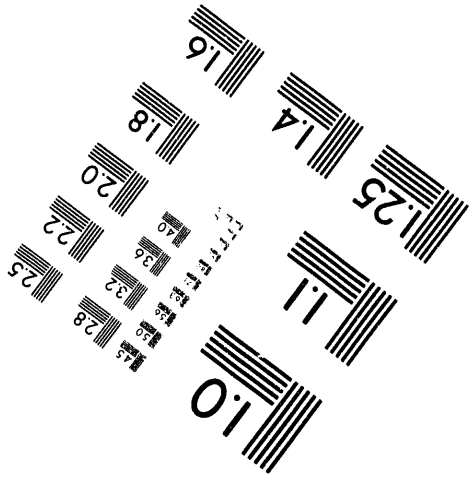

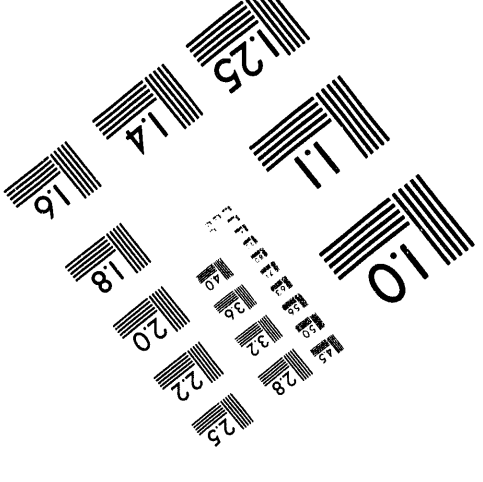

MANUFACTURED TO AIIM STANDARDS
BY APPLIED IMAGE, INC.

1 of 1

ANL/RE/CP--80782
Conf-940752--5

MITIGATION OF EARTHQUAKE HAZARDS USING SEISMIC BASE ISOLATION SYSTEMS

C. Y. Wang[1]

Abstract

This paper deals with mitigation of earthquake hazards using seismic base-isolation systems. A numerical algorithm is described for system response analysis of isolated structures with laminated elastomer bearings. The focus of this paper is on the adaptation of a nonlinear constitutive equation for the isolation bearing, and the treatment of foundation embedment for the soil-structure-interaction analysis. Sample problems are presented to illustrate the mitigating effect of using base-isolation systems.

Introduction

Seismic isolation represents a significant engineering breakthrough in structural designs, due to its capabilities of protecting structures and their contents from earthquake damage. One main concept in base isolation is to reduce the fundamental frequency of structural vibration to a value lower than the energy-containing frequencies of earthquake ground motions. The other purpose of an isolation system is to provide a mechanism for energy dissipation and to reduce the accelerations transmitted to the superstructure. In other words, by using base-isolation devices at the foundation of a structure, the structure is essentially decoupled from the ground motion during earthquakes.

In order to simulate the bearing behavior under earthquakes, a nonlinear viscoelastic constitutive model is utilized. This formulation requires six input parameters derived from experimental data of the bearing under sinusoidal loading. The characteristic behaviors of the isolation bearing, such as the variation of shear modulus and material damping with the change of maximum shear deformation, are captured quite closely by the formulation.

---

[1]Civil Engineer, Reactor Engineering Division, Argonne National Laboratory, Argonne, IL 60439.

Since structural response also depends significantly upon the input acceleration time histories acting on the foundation level, a soil analysis is performed to evaluate the foundation input motion as well as the stiffness and damping of the soil deposits. The analysis further accounts for isolator nonlinearities, foundation embedment, and inertia and kinematic interaction between the soil and structure.

The viscoelastic constitutive model and soil-analysis capability have been incorporated into a three-dimensional system response program, SISEC (Seismic Isolation System Evaluation Code), developed at Argonne National Laboratory (ANL). In this paper, response simulations of base-isolated structures are carried out with the SISEC code using the time-history method. Validations of numerical simulations with actual earthquake observation data are also presented. Furthermore, relative responses of isolated and nonisolated structures are investigated.

Results of the observation data and numerical analyses prove that the base-isolation system is advantageous. In general, accelerations at the highest locations of the isolated structures are only 20% to 30% of the ordinary structure accelerations. Also, results of one example reveal that for both ordinary and base-isolated buildings, the computed accelerations agree reasonably well with those recorded.

Analytical Developments

Nonlinear Constitutive Model

The relationship between the applied displacement at one end of the elastomer bearing and the corresponding resultant force at the other end is essential for seismic analysis. This type of relationship under shear loading of composite isolation bearing has been successfully reproduced at ANL. The constitutive relation for viscoelastic material usually involves the deformation gradient denoted by F. By polar decomposition, the deformation gradient in turn can be directly related to the right Cauchy-Green tensor C, as follows:

$$C = F^{T}F \ , \tag{1}$$

where the superscript T designates the transpose of a matrix. This tensor measures pure deformation. Similarly, with J denoting the determinant of F, the volume-preserving right Cauchy-Green tensor is given as

$$\bar{C} = CJ^{-2/3} \ . \tag{2}$$

In the viscoelastic constitutive formulation (Simo and Taylor, 1985), the volumetric response of the material is assumed to be purely elastic; the viscoelastic effects are embodied by the deviatoric component. Their formulation is related to the second Piola-Kirchhoff stress tensor σ. The basic Simo-Taylor (S-T) constitutive model is expressed as a convolution integral of the form

$$\sigma(t) = K \ln J + \int_0^t \mu(t-s)\, \dot{\pi}\left[e(s), \varphi_t\right] ds \ , \tag{3}$$

where the first term on the right-hand side of Equation 3 represents the volumetric component of stress and the second term stands for the deviatoric component. The bulk modulus K and the determinant of F (or det F) finalize the volumetric expression of the stress formulation.

Through a judicious selection of the nonlinear functions conforming to the physical material response of highly filled polymers, the solution of Equation 3 replicates many of the characteristics of seismic bearings in shear under sinusoidal excitation. This was substantiated by a parameter study of the constitutive relation (Kim, et al., 1991).

Note, the original S-T constitutive relation for shear loading requires five input parameters. However, we have found from many numerical experimentations that a modified S-T constitutive model involving six parameters yields better results. In the modified model shown in Figure 1, the first five parameters are derived from experimental plots of storage and loss moduli, the initial shear stiffness plus stiffness at very large strain, as well as the relaxation tests. The sixth parameter pertains to the weight ratio of the original relation to the nonlinear variable resistance in parallel.

Soil-structure interaction

A three-step spring method (Kausel, et al., 1978) is adapted for the soil-structure interaction (SSI) analysis to treat a structure with deep foundation embedment and highly nonlinear isolation system. The first step calculates the foundation input motions (translation and rotation). The second step evaluates the impedance functions for the embedded foundation. The third step uses the foundation input motion and impedance function as input for the SISEC code to perform the detailed SSI analysis.

Due to the presence of embedment, the foundation experiences not only horizontal translation motion, but also the rocking motion for a purely horizontal free-field motion. These horizontal and rocking motions, denoted by $X_i(t)$ and $\varphi_i(t)$, respectively, are given by:

$$\ddot{X}_i(t) = \mathrm{IFT}\begin{cases} \ddot{X}_g(\omega)\left[\cos\left(\frac{\pi}{2}\,\frac{f}{f_n}\right)\right] & \text{if } f \le 0.7\ f_n \\ \ddot{X}_g(\omega)[0.453] & \text{if } f > 0.7\ f_n \end{cases}$$

and (4)

$$\ddot{\phi}_i(t) = \mathrm{IFT}\begin{cases} \ddot{X}_g(\omega)\left[0.257\left(1 - \cos\frac{\pi}{2}\,\frac{f}{f_n}\right)/R\right] & \text{if } f \le 0.7\ f_n \\ \ddot{X}_g(\omega)[0.257/R] & \text{if } f > 0.7\ f_n \end{cases}$$

where IFT stands for Inverse Fourier Transformation; $X_g(\omega)$ is the Fourier transform of the horizontal acceleration at the free surface in the free field, and f_n is the fundamental shear frequency of the embedment region.

To evaluate the impedance functions, we assume the structural foundation is embedded in a homogeneous stratum. Let F and M be the horizontal force and rocking moment at the interface of the foundation and soil, and X and ϕ be the corresponding lateral and rocking displacements, respectively; then F and M are related to X and ϕ through the impedance functions. These relationships can be mathematically written as

$$\begin{Bmatrix} F \\ M \end{Bmatrix} = \begin{bmatrix} K_{xx} & K_{x\phi} \\ K_{x\phi} & K_{\phi\phi} \end{bmatrix} \begin{Bmatrix} X \\ \phi \end{Bmatrix}, \tag{5}$$

where K_{xx} $K_{x\phi}$, and $K_{\phi\phi}$ are the impedance functions. These coefficients generally are functions of the soil shear modulus, radius of the foundation, depth of the embedment, and the depth of bedrock, soil Poisson's Ratio, etc. (Kausel, et al., 1978).

Results and Discussions

Response Analyses of Reinforced Concrete Buildings

Two test buildings, one conventionally designed and the other base-isolated, were constructed side-by-side at Tohoku University in Sendai, which is located in the northern part of Japan. The test buildings consist of two full-size, three-story reinforced concrete structures as shown in Figure 2. The dimensions and construction details of the superstructures were exactly the same for both buildings.

The isolation system of the base-isolated building consists of six identical bearings designed with a medium shape factor and molded with a high damping, low shear modulus rubber. These bearings are laminated composites with 12 layers of rubber and 11 layers of steel plates (shims) manufactured by Rubber Consultants, UK.

Three-dimensional frame models are used in numerical simulations for both ordinary and base-isolated buildings. In the analysis, beams, columns, and girders are all modeled by 3-D beam elements with six degrees of freedom per node, to account for the translations and rotations generated from seismic events. Stiffnesses of the outer walls and partitions that are not structurally connected to the beams and girders are neglected in the calculation. However, their masses are appropriately lumped to the element nodal points, so that their inertia effects are included in the analysis.

The mathematical models of both ordinary and base-isolated buildings are given in Figure 3. These two models are almost identical except that different modeling techniques are used for the substructure connecting the basement slab and the first floor. Specifically, the major difference (in the models) is in the middle portion of the support columns where the isolator is

located. For the ordinary building, each basement column is represented by three beam elements. For the isolated building, on the other hand, the isolator is modeled by two spring elements; one linear spring and one nonlinear spring to simulate, respectively, the vertical and horizontal responses of the isolator. Two beam elements, similar to those columns of the superstructure are then utilized above and below the isolator to model the reinforced concrete pedestals.

In simulating the responses of ordinary and isolated buildings, the X (transverse) and Y (longitudinal) direction accelerations observed at the center of the basement of the isolated building are utilized as input to the basement structural nodes. The computed accelerations are then compared with the recorded observations. Here a representative earthquake (#42) is chosen for the numerical simulation. This earthquake had the strongest ground motion among seven earthquakes observed at the test facility (Kuroda, et al., 1991).

For simplicity, comparison of observed and calculated peak accelerations at the first floor and the roof level of both the ordinary and isolated buildings are given in Table 1. As seen from this table, the maximum accelerations obtained from recorded data and SISEC simulations agree satisfactorily with each other. In fact, the deviation between the calculated and observed accelerations at both the first floor and the roof levels of the isolated building is within 21%.

To study the effectiveness of the base-isolation system, Table 1 further lists the acceleration ratio, i.e., the acceleration of the isolated building A_I, divided by the acceleration of the ordinary building A_O. The advantage of the base isolation system in mitigating the seismic response is quite evident. For earthquake #42, the simulated transverse acceleration at the first floor of the isolation building is about 54% of the ordinary building, whereas in the recorded data it is about 66%. At the roof level, the advantage of base isolation becomes more evident. The analytical results indicate that, in the transverse and longitudinal directions, the accelerations of the isolated building are about 23% and 27% of the ordinary building accelerations, respectively. In the observation data the acceleration ratios are about 26% and 33%, respectively. This further demonstrates that as the floor elevation increases, the degree of acceleration reduction also increases.

To illustrate the effect of the isolation system, Figure 4 compares both observed and calculated accelerations in the transverse direction at the roof level. As can be seen, the peak accelerations are greatly reduced for the isolated building.

Response Analyses of Nuclear Structures

The finite-element model of a nuclear facility is shown in Figure 6. Two lumped-mass sticks are used to model the reactor containment and reactor building. Two calculations are performed dealing with unisolated and isolated plants, respectively. For the unisolated plant, one foundation mat is utilized. On the other hand, the isolated plant has two concrete foundation mats, and the isolators are placed between these two mats. The design fundamental frequency of the isolators is 0.50 Hz. The free-field artificial input acceleration history has a peak ground acceleration of 0.20 g.

In calculating the response of the isolated structure, the isolators are modeled by two spring elements, one linear spring for simulating the large vertical stiffness and one nonlinear viscoelastic spring for modeling the relatively low stiffness in the horizontal direction. For simplicity, only one composite isolator representing the global effect of the estimated 600 isolators is used in the analysis. The input parameters of the horizontal nonlinear spring using the viscoelastic constitutive model were based on experimental data of 1/4-scale PRISM-type bearings (Tajirian and Kelly, 1988) and have these values: $G_0 = 250$, $G_\infty = 55$, $\nu = 0.35$, $\alpha = 0.10$, $\beta = 0.30$, $C = 0.55$.

Maximum accelerations at node 1 (basemat), 23 (top of containment) and 43 (top of the reactor building) are useful for studying the relative merit of the high damping base-isolation system. For the unisolated plant, the peak accelerations of these three locations are 0.22 g, 0.43 g and 0.33 g.

However, for the isolated structure, the maximum accelerations at nodes 1, 23, and 45 are about 0.083 g, 0.0875 g, and 0.085 g, respectively. Note that because of softness of the isolator bearings in responding to the horizontal excitation, the peak accelerations at these three locations are much smaller than that of the input ground acceleration, 0.20 g. In other words, by using the high damping elastomeric bearings, the superstructure is basically decoupled from the ground motion during the earthquake. For illustration of the mitigating effect of elastomer bearings, comparison of acceleration histories at node 23 (top of the reactor containment) of the unisolated and isolated plants is given in Figure 6. Figure 7 displays the hysteresis plots of the composite bearing. The energy absorbed by the bearing is shown in Figure 8.

Acknowledgments

The author would like to thank Dr. Y. Tang and Professor A. H. Marchertas for their assistance. This work was supported jointly by the U.S. Department of Energy and the National Science Foundation under contracts W-31-109-Eng-38 and CES-8800871, respectively.

References

Kausel, E., et al., "The Spring Method for Embedded Foundations," *Nucl. Engrg. & Design*, 48, (1978), North-Holland, 377-392.

Kim, M., et al., "Utilization of the S-T Viscoelastic Constitutive Model for the Simulation of Isolation Bearing," *Trans. 11th International Conference on Structural Mechanics in Reactor Technology (SMiRT-11)*, paper K23/4, 1991, Tokyo.

Kuroda, T., et al., "Outline of Study and Test on Characteristics of Individual Bearing," Report No. ANL/Shimizu, SHUM-006, Rev. 0, June, 1991, Argonne National Laboratory, Tokyo.

Simo, T. and Taylor, R., "A Three-Dimensional Finite Deformation Viscoelastic Model Accounting for Damage Effects," Report No. UCB/SESM/85-02, SESM, University of California, Berkeley, 1985.

Tajirian, F. and Kelly, T., "Testing of Seismic Isolation Bearings for Advanced Liquid Metal Reactor PRISM," ASME Special Publication, PVP-Vol. 147, 1988.

Table 1. Comparison of accelerations of ordinary and isolated buildings (earthquake #42)

Location	Direction	Ordinary Building, A_o		Isolated Building, A_I		Accel. Ratio, A_I/A_o	
		Obs. gal	Cal. gal	Obs. gal	Cal. gas	Obs.	Cal.
Roof	T(X)	7.18	6.96	1.87	1.59	0.26	0.23
	L(Y)	7.29	7.16	2.46	1.94	0.33	0.27
First Floor	T(X)	2.10	2.45	1.39	1.33	0.66	0.54
	L(Y)	2.79	3.58	1.90	1.70	0.68	0.47
Basement	T(X)			2.19			
	L(Y)			2.70			

T: Transverse L: Longitudinal

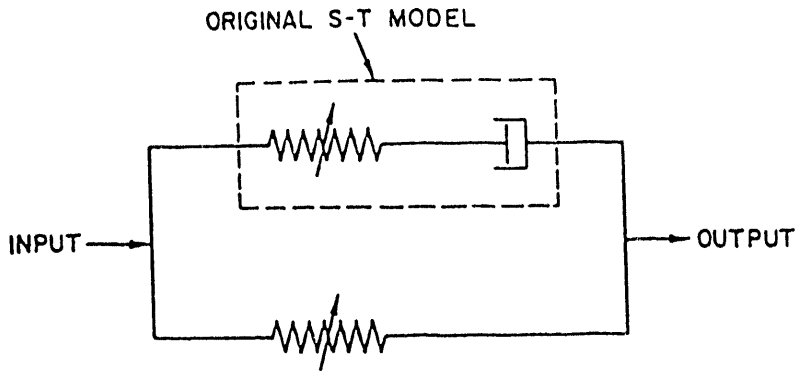

Figure 1. Modified S-T constitutive model

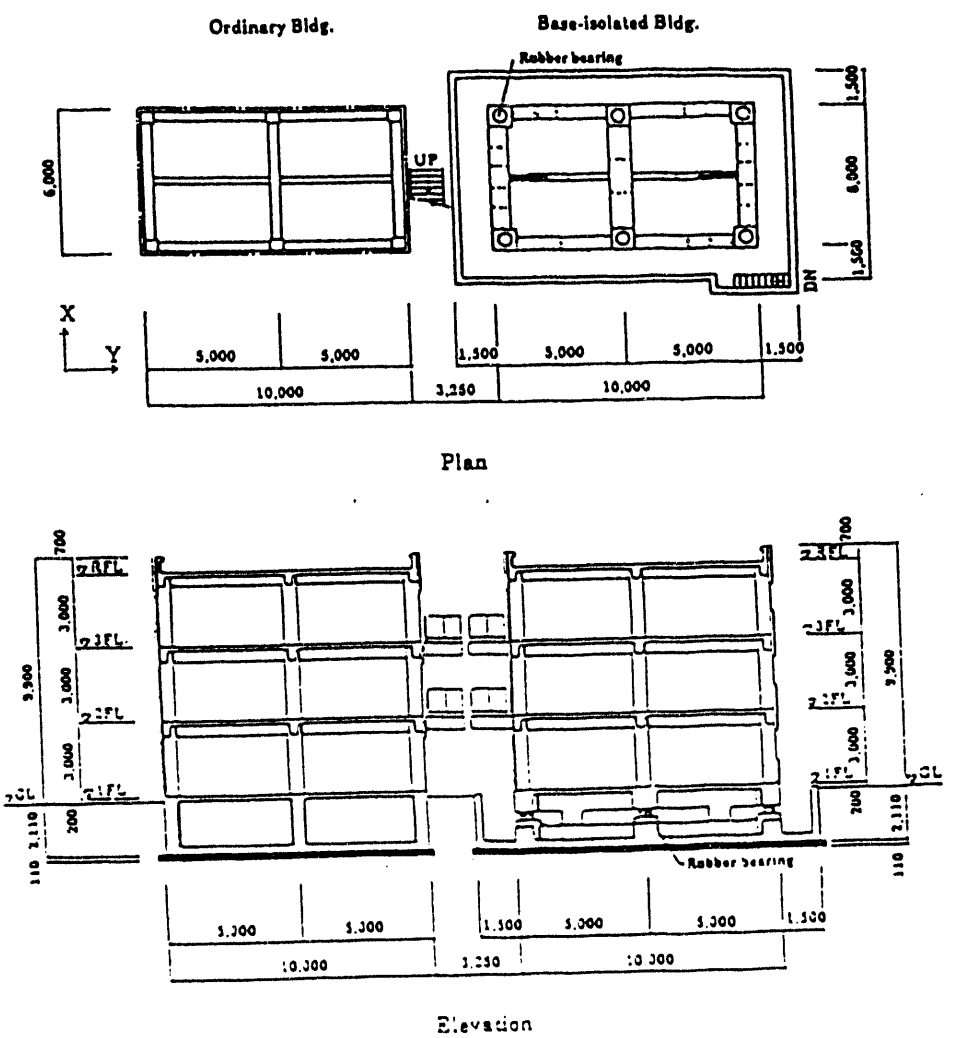

Figure 2. Plan and elevation of test building.

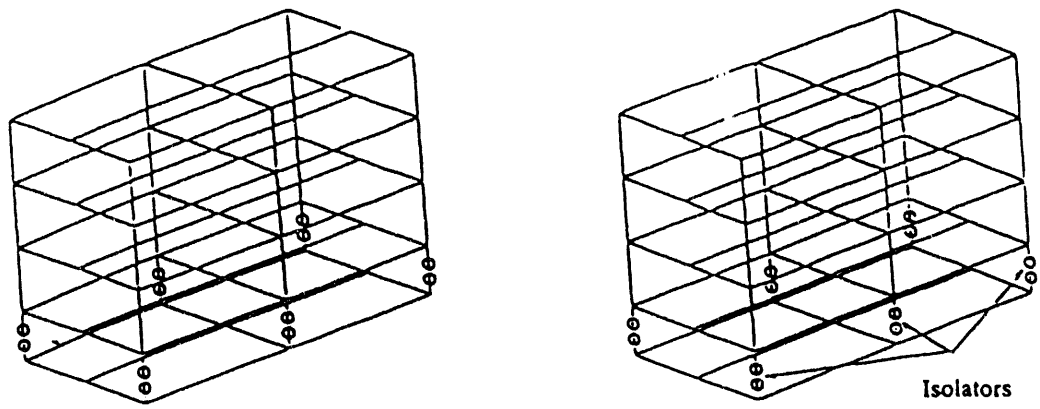

Figure 3. Mathematical model of ordinary and isolated buildings.

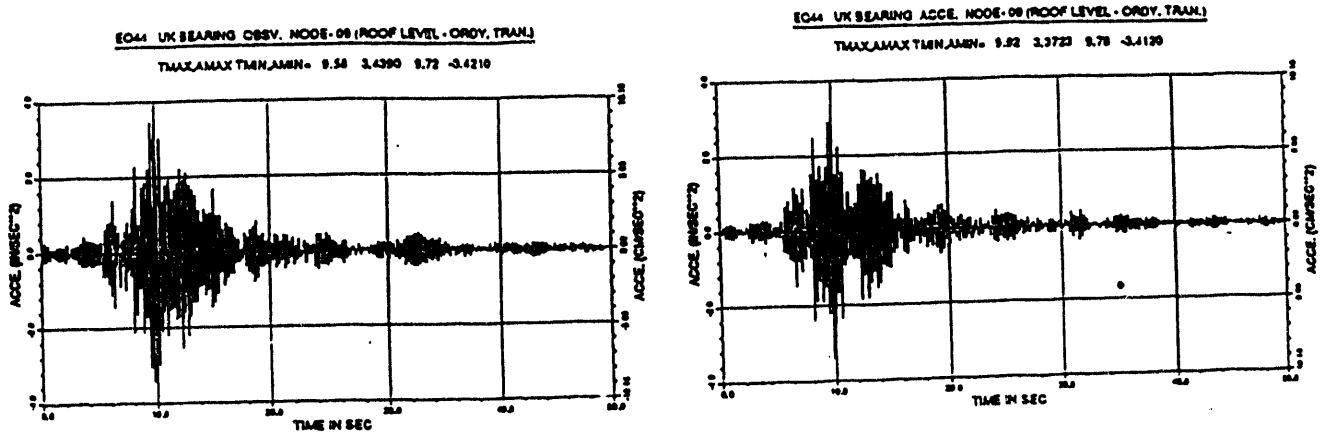

Ordinary Building

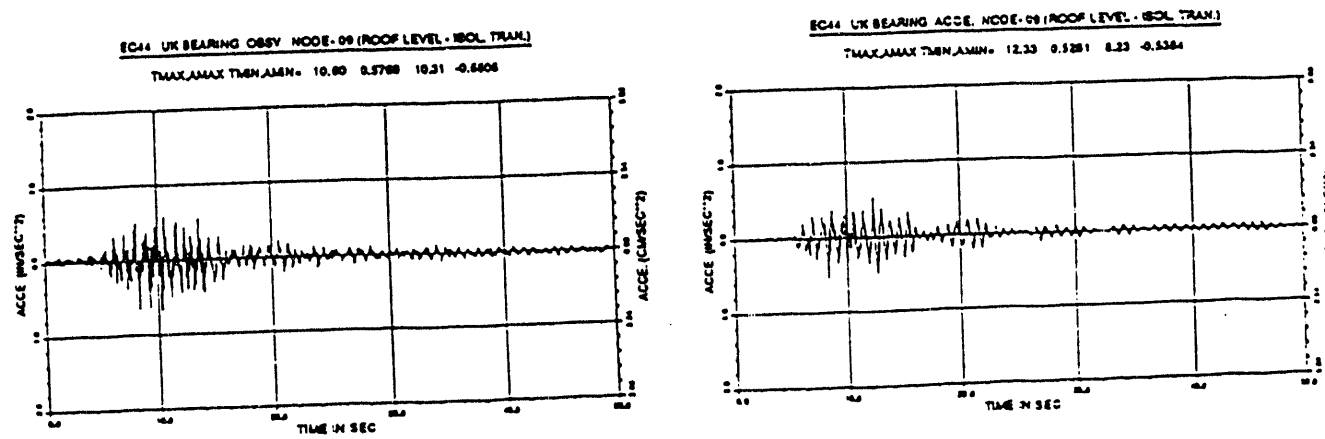

Isolated Building

Figure 4. Comparison of observed and calculated transverse accelerations at the roof level (left: observed, right: calculated).

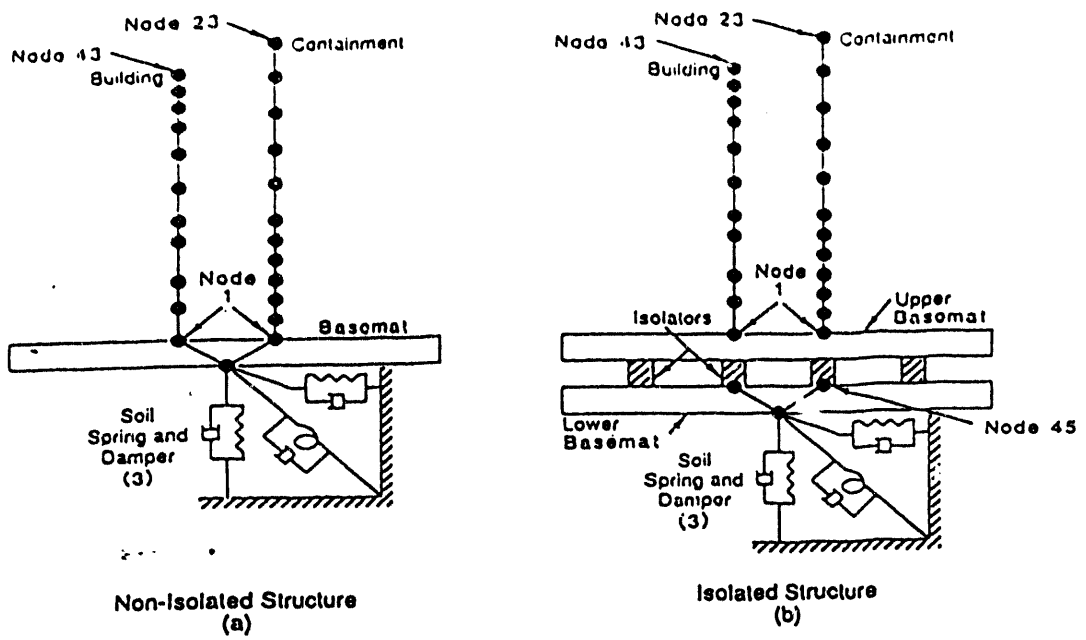

Figure 5. Finite-element model of a nuclear facility.

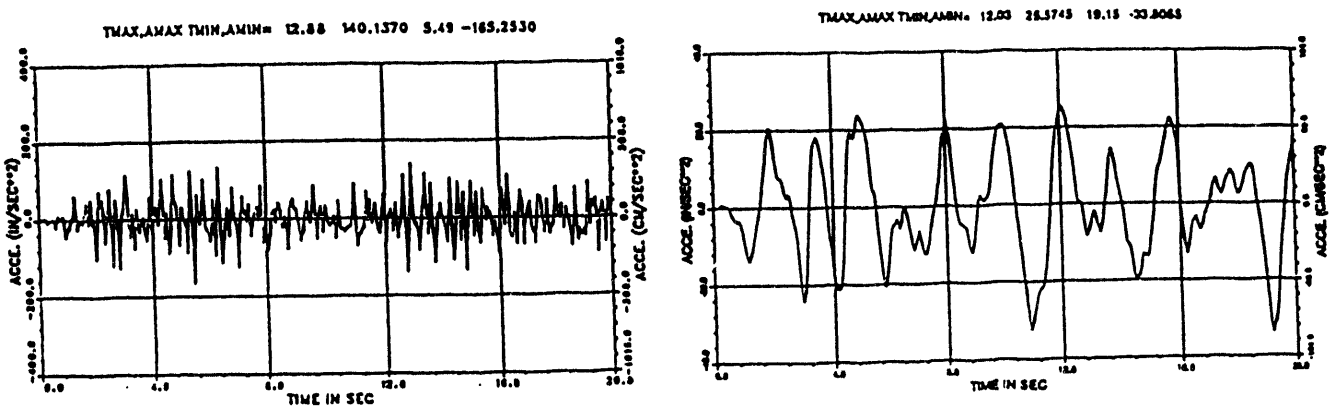

Figure 6. Acceleration histories at the top of containment (left: unisolated, right: isolated).

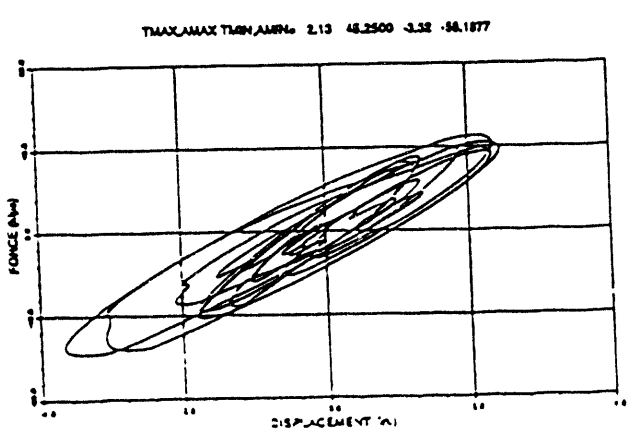

Figure 7. Hysteresis loop of a composite bearing.

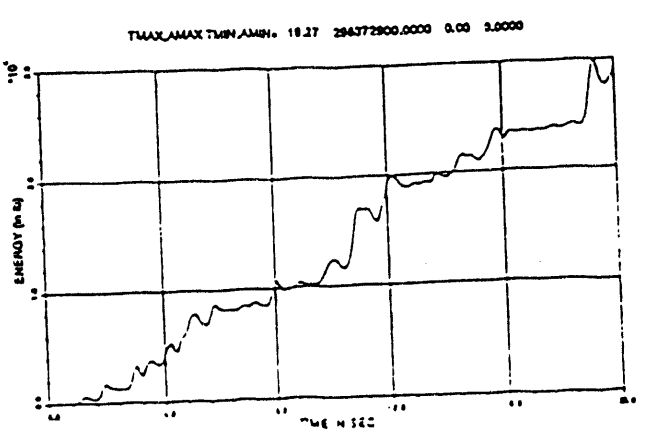

Figure 8. Energy absorbed by the bearing

DATE
FILMED
8/17/94
END